ENHANCEMENT OF SYNTHETIC APERTURE FOCUSING TECHNIQUE (SAFT) BY ADVANCED SIGNAL PROCESSING

M. Jastrzebski, T. Dusatko, J. Fortin, F. Farzbod, A.N. Sinclair; University of Toronto, Toronto, Canada; M.D.C. Moles; R-D Tech, Mississauga, Canada; F. Honarvar; KNT University of Technology, Tehran, Iran.

Abstract: The synthetic aperture focusing technique (SAFT) is a well-established method for improving the resolution of an ultrasonic image. A major shortcoming is the inherent assumption that the pulse reflected from a flaw has a spectral content that is independent of the flaw's location relative to the transducer. In this project, we address the issue by using SAFT combined with Wiener filtering and an angle dependant set of reference signals. This allows the image of the flaw to be reconstructed with less distortion. The signal processing schemes are applied to synthetic flaw signals, and then to real defects of the type found in girth welds of gas pipelines. The result is a marked sharpening of both lateral and depth resolution, such that time-of-flight calculations can be used to obtain accurate measures of defect height.

Introduction: Ultrasonic nondestructive testing (NDT) is employed primarily in the detection of critical defects within mechanical or structural components. For safety and economic reasons, it is of great importance to be able to size flaws accurately. SAFT is a signal processing tool that aim at improving the accuracy of ultrasonic signals, thus leading to better sizing capabilities. SAFT synthesizes a large focused transducer by gathering data at various positions using a small unfocused transducer. A synthetic aperture focusing system will produce a narrow synthetic beam by the mean of a coherent summation of phase adjusted pulses (A-scans). Since the synthetic beam width is much smaller than the actual transducer beam width, SAFT greatly improves the lateral resolution and the signal-to-noise ratio of the raw B-scan.

A way of improving the temporal resolution is to deconvolve the A-scans before applying the SAFT algorithm. Wiener filtering is known to be one of the most effective deconvolution techniques [1]. The backwall echo is usually used as a reference signal. In this paper we refer to this technique as SAFTD. SAFTD is essentially an application of SAFT processing on an image which has been deconvolved with a single, on-axis reference signal. It is a well known fact that the lower frequency components of a beam have a wider divergence angle than the higher frequency components. This fact can be visualized in figure 1 which shows the on-axis frequency spectrum of a ultrasonic beam superposed on its frequency spectrum at an angle of 15˚.

Figure 1: Frequency spectrum of a transducer at two different values of θ

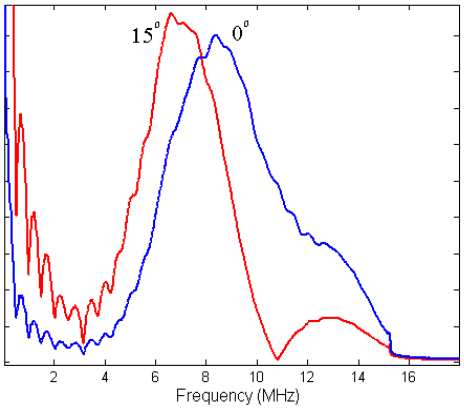

The use of the on-axis signal as a reference for deconvolution becomes inappropriate when θ is large since the frequency spectrum is shifted toward the low frequencies. One way to tackle this problem is to use an angle dependent deconvolution technique in conjunction with SAFT

(SAFTADD). The SAFTADD operates in close analogy to the SAFT. However, instead of using the raw measurement data to generate the corrected image, it deconvolves each A-scan with the angle-corrected reference signal. To accomplish this in a computationally efficient fashion, a set of reference signals is first generated by a numerical model for a range of oblique angles. The raw B-scan is then deconvolved with each reference signal in this set to generate a library of B-scans, each deconvolved with a signal corresponding to an oblique angle. Each uncorrected point becomes a function of t, and x as before, but also of θ, the angle of the reference signal with which the raw point was deconvolved (Figure 2). Modifying the SAFT scheme to take this into account yields SAFTADD.

Figure 2: Schematic representation of SAFT using a θ dependent deconvolved B-scan

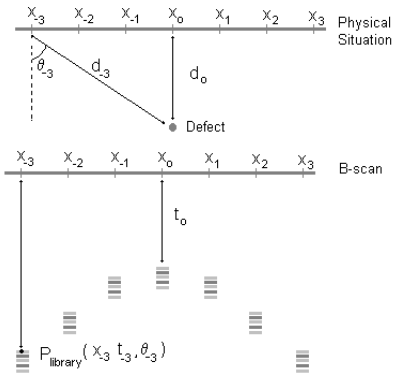

The performance of SAFTADD is first evaluated under ideal conditions. To this end, a comparison between SAFT/SAFTD and SAFTADD was done on synthetic data which simulated a B-scan collected with a typical pulse-echo inspection system. The data was generated synthetically using the numerical model. The second set of tests aimed to determine whether the results of the first study would be duplicated under more realistic conditions with data collected experimentally.

Results: SAFTADD implies that each A-scan must be deconvolved using an appropriate reference signal according to its angle of divergence θ. We thus need a numerical model than will generate these reference signals. This model, based on the application of Huygen's principle and ray theory, can predict the displacement field produced by a piston transducer inside a sample. Figure 3 presents an example of the configuration and the coordinate system used for the calculations.

Figure 3: Representation of a circular piston transducer

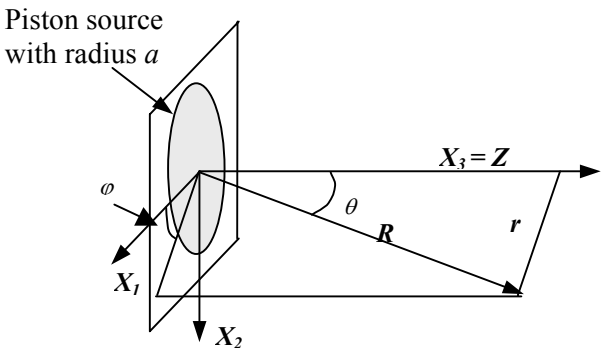

Since an experiment that we carried out has shown that the ultrasonic beam was symmetric at the frequencies commonly used in NDT, we can neglect the dependence on φ and the wavefield is going to be a function of R and θ only. For a uniformly excited transducer, the radial displacement can be expressed by the following relation:

$$u_R = \frac{a^2 \sigma_{zz}}{4\pi\mu} \frac{exp(-ik_\alpha R)}{R} \times \left[\frac{2J_1(k_\alpha a \sin\theta)}{k_\alpha a \sin\theta}\right] \frac{(\beta/\alpha)^2 \cos\theta [1 - 2(\beta/\alpha)^2 \sin^2\theta]}{[1 - 2(\beta/\alpha)^2 \sin^2\theta]^2 + 4(\beta/\alpha)^3 \sin^2\theta \cos\theta [1 - (\beta/\alpha)^2 \sin^2\theta]^{1/2}}$$

where α is the pressure wave velocity, β the shear wave velocity, k_α the pressure wave number and σ_{zz} the stress at the surface of the transducer [2]. Since σ_{zz} is unknown, the program does not calculate the absolute value of the displacement field but the relative displacement normalized by the experimental spectrum obtained at θ = 0˚. The total displacement at one point is obtained by summing up the displacements caused by several concentric circular transducers. This approach is required because the transducer surface does not vibrate uniformly. The contribution of each concentric transducer is weighted by an appropriate factor. These weights have been determined experimentally. The program that was developed was used to create the necessary libraries of signals by using an appropriate on-axis reference obtained experimentally. Each library is composed of signals covering the range θ = 0-24.5º in half-degree increments. The range and increments were selected to be sufficient based on geometric consideration of the lateral step size, the defect depth, and the transducer characteristics.

The first part of the experimental work is the synthetic signal study. The values of the parameters in the synthetic study are similar to the experimental values in the second part of the experiment. The transducer that was used had a 7.5 MHz central frequency and a 3 mm diameter. The defect was located in the far field. The synthetic B-scan images were constructed by first computing an appropriate time-delay and corresponding transducer angle at each lateral scan position to the left and right of the synthetic defect location (see figure 2). The angle to the pixel under consideration was used to select the appropriate corresponding signal from the synthetic library. The correct time-delay was then applied to the signal, and the signal inserted into the image. This procedure is analogous to applying the SAFT in reverse at a single point, and at each scan location, inserting a correctly selected signal. Once the synthetic B-scan images were created, they were processed with SAFT, SAFTD and SAFTADD. The signal library used to generate the synthetic images was also used as the reference signal library for the SAFTADD. To maintain consistency, the 0^o signal from the reference library was used as the reference for the deconvolution step of SAFTD.

Figure 4 presents the processed images of the synthetic defect. We notice that SAFTD improves the temporal resolution and SAFTADD significantly improves the lateral resolution as well as the temporal resolution. The images obtained by SAFTADD however contain numerous artifacts. The images presented in figure 4 have subsequently been treated by determining the analytic signal magnitude. The 6 dB drop signal envelope can thus be drawn. This allows size measurements to be made directly on the image. The results obtained are presented in table 1.

Figure 4: SAFT, SAFTD and SAFTADD Processing of Synthetic Images

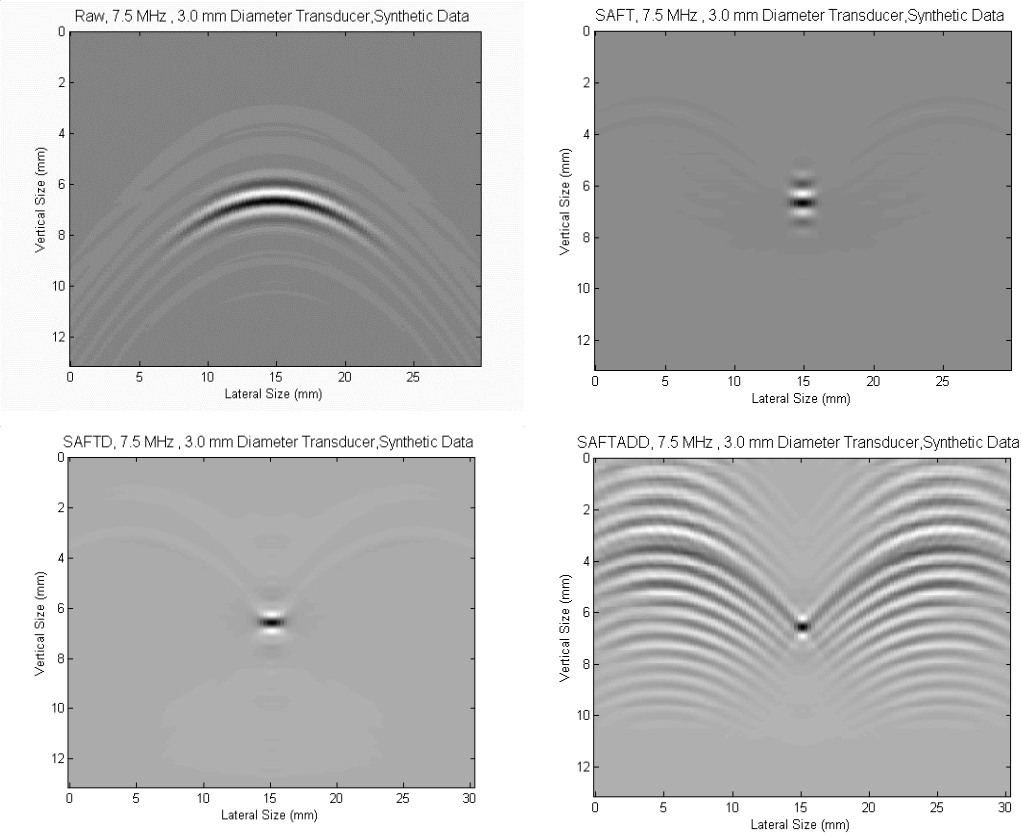

Table 1: Horizontal and vertical size measurements for synthetic results

	Synthetic	
	Vertical Size (mm)	Lateral Size (mm)
SAFT	1.05	1.25
SAFTD	0.68	1.25
SAFTADD	0.67	0.75

The specimen used for the experimental data collection is a 44.5x44.5x162mm aluminum block. The artificial defect is a 2mm diameter side-drilled through-hole, located 31.5mm from the test-surface of the block (Figure 5). The hole diameter was chosen to be the smallest possible, under machining constraints. It is assumed that this hole acts as a perfect reflector. The apparatus used to generate the B-scan image is a two-axis immersion scanner located in the University of Toronto Ultrasonic NDE Laboratory. The scanner is equipped with a motion controller and is coupled to a PC through a digitizer. Winspect^{TM} NDE software was used to display and process the collected data. The same processing parameters were used in order to maintain as close a correspondence as possible between the two studies. Figure 6 and table 2 present the results obtained from the experiment.

Qualitative examination of the SAFT, SAFTD and SAFTADD-processed experimental data reveals results very similar to those produced by the synthetic study. The pattern of artifact formation is almost identical, although the artifacts seem more strongly defined. There is also an obviously stronger noise component than that found in the synthetic study, but this is due to the non-ideal conditions under which the experiment was carried out.

Figure 5: Aluminum Test Block with 2mm Side-Drilled Through-Hole Defect

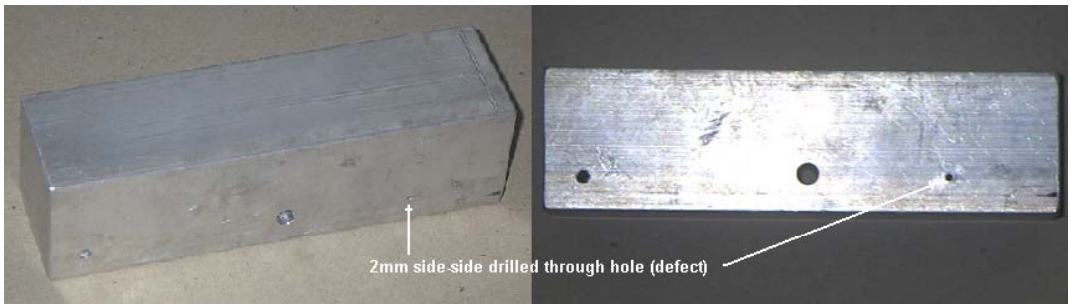

Figure 6: SAFT, SAFTD and SAFTADD Processing of Experimental Images

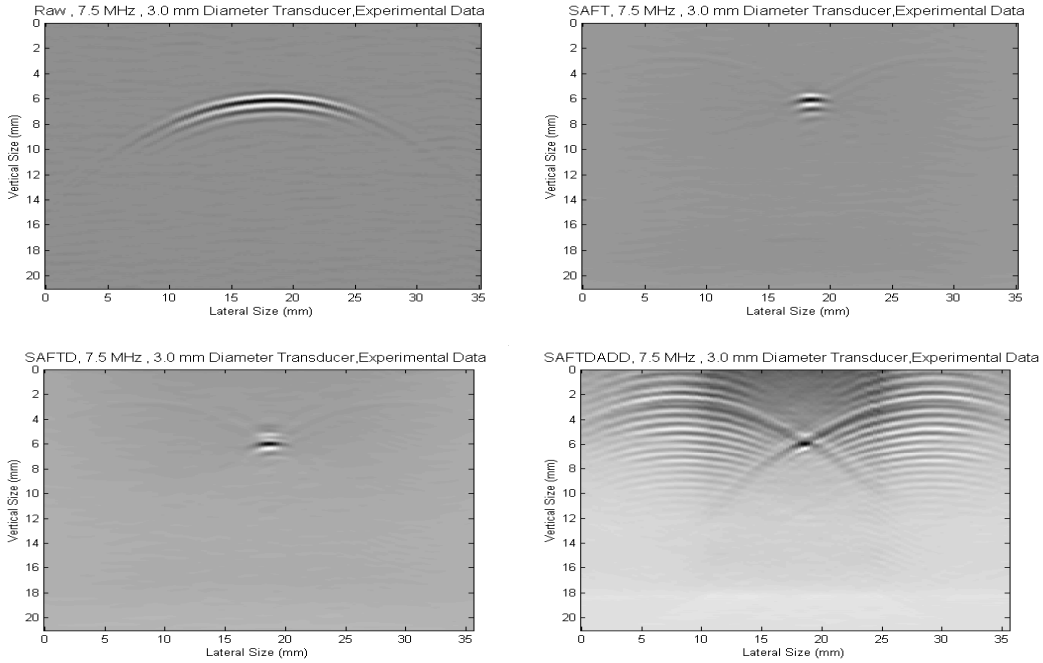

Table 2: Horizontal and vertical measurements for Experimental results

	Experimental	
	Vertical Size (mm)	Lateral Size (mm)
SAFT	1.22	1.75
SAFTD	0.64	3.25
SAFTADD	0.77	1.75

Discussion: The synthetic data study aimed to accomplish two goals: the first was to determine whether the SAFTADD was capable of producing significant improvements in resolution over SAFT and SAFTD, and the second was to quantify the degree of improvement which could ideally be achieved. In the case of the synthetic study it is apparent that, by accounting for the angle-dependence of frequency content, the SAFTADD was able to produce a significant local improvement in lateral resolution over the traditional SAFT and the SAFTD. The reported horizontal resolution with both SAFT and SAFTD treatment is 1.25mm (see table 1 and figure 4).

SAFTADD is able to improve this by 40% to 0.75mm, which correspond to ¼ of the transducer diameter. This corresponds to the theoretical limit of the resolution of SAFT when the resolution is defined as being the full width at half amplitude of the synthetic beam [3]. Both SAFTD and SAFTADD show a considerable (~35%) improvement in temporal resolution over traditional SAFT. This is the result of the artificial bandwidth increase introduced by deconvolution. A comparison of Table 1 representing the synthetic results, and Table 2 representing the experimental results shows a significant difference between the two studies. The main difference is the horizontal size reported by the experimental study, which is significantly larger than that reported in the synthetic study. This is believed to be largely caused by the increased presence of artifacts that blur the signal.

The mechanism by which the artifacts are formed during SAFTADD processing is very similar to that responsible for the formation of side lobes in traditionally SAFT-processed images. The main difference lies in the fact that deconvolution greatly aggravates the problem by creating simultaneously stronger and more temporally extensive signals on which the mechanism may act. The heart of the problem lies in the presence of nulls in the off-axis (high-angle) signals used for deconvolution (Wiener Filtering). When such signals are used to deconvolve a signal where the null is not present, the resultant signal is dominated by a large delta-like peak at the null frequency. This situation is most likely to occur when an off-axis reference signal is used to deconvolve an on-axis signal. Figure 7 shows a B-scan deconvolved with a reference signal corresponding to a transducer position 10^{o} from the defect location. The image clearly shows that A-scans located close to the axis of the defect exhibit "ringing" at the null frequency of the reference signal.

Figure 7: Result of filtering with incorrect off-axis reference signal

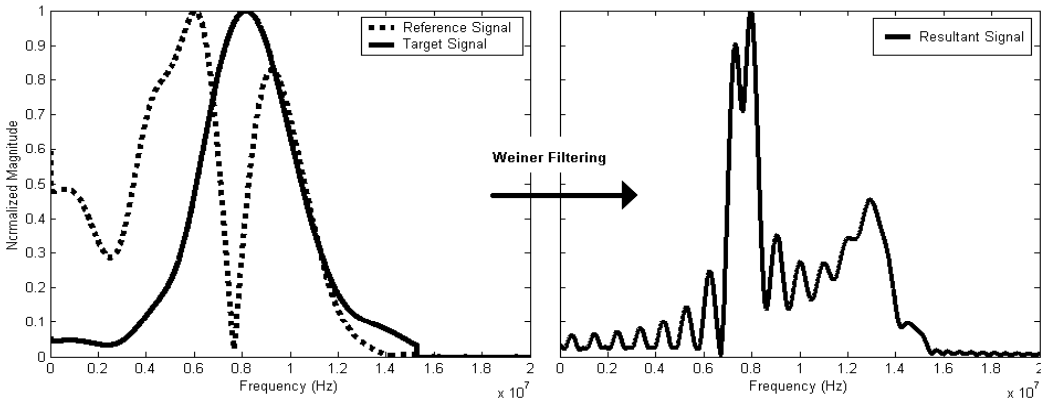

Conclusions: A synthetic aperture focusing technique with angle-dependent deconvolution was developed by combining a time-domain SAFT scheme with Wiener filtering and an angle dependence model. The technique was evaluated both on synthetically generated, and experimentally collected data. The synthetic data study concluded that the SAFTADD was significantly better than the SAFT or SAFTD at improving the lateral and temporal resolution of B-scans. It was also found that the algorithm introduced high levels of artifacts into the processed image. The experimental data was largely in agreement with the synthetic-data study on the level of depth resolution improvement. However, the level of lateral resolution improvement was not echoed in the experimental study. Accurate measurements of resolution were made difficult by the presence of much stronger artifacts. This increase in artifact strength is believed to be caused by noise in the non-ideal images of the experimental data study.

Areas of future work include tuning the algorithm in order to obtain artifact-free images. The numerical model could also be modified to include a two probes configuration, which would

enable its use with TOFD. The SAFT algorithm could also be modified in order to account for the finite size of the transducer.

References:

1- Sam-Kit Sin, Chi-Hau Chen, "A comparison of deconvolution techniques for the ultrasonic nondestructive evaluation of materials," *IEEE Transactions on Image Processing*, Vol. 1, No. 1, Jan. 1992.

2- Tang, X.M., Zhu, Z., Tokoz, M.N., "Radiation patterns of compressional shear transducers at the surface of an elastic half-shape", *J. Acoust. Soc. Am*., 95(1), 1994, 71-76

3- Thomson, R.N., "Transverse and longitudinal resolution of the synthetic aperture focusing technique" *Ultrasonics*, 9-15, Jan 1984